

II. RESULTS OF A MATHEMATICAL EXPERIMENT

V. N. Vasil'ev, G. N. Dul'nev,
and V. D. Naumchik

UDC 621.365.3

An optimization algorithm is examined for the construction of the heating element of a resistive furnace for drawing optical fibers, and results of a numerical experiment are presented.

The resistive electrical furnaces with graphite heating elements utilized at this time for the industrial production of optical fiber [1-3] have the following features.

1. A short heater lifetime (50-100 h). Let us note that its exploitation time depends on the maximal working temperature in the heating zone and on its distribution along the surface [4].

2. A high temperature in the domain of ingot heating results in the intensive formation of dust particles of the materials (diameter on the order of 2 μm) from which the furnace components are executed. The particles falling on the melted part of the ingot or on the fiber surface cause the appearance of microcracks, i.e., degradation of the quality of the optical fiber being drawn occurs, the dust particle concentration in the heating zone is proportional to the maximal working temperature of the heating element [5].

3. The most gradual ingot heating occurs in resistance furnaces as compared with other possible heating methods, resulting in the formation of the most extensive deformation domain [6]. The stability of the optical fiber drawing process diminishes here and its reaction to the external disturbing effects is increased [7].

The resistance furnace heating features listed above suggest the means and methods for their optimization. Increasing the graphite heater element lifetime and diminution of the dust particle concentration in the heating zone are possible by lowering the maximal working temperature of its surface [8, 9]. Since the heat transfer in the heating zone is primarily radiational, then the problem posed can be solved by selecting the generatrix of the internal heating surface in such a way as to assure the maximal value of the angular radiation coefficients on the surface of the quartz glass melt.

Theoretical investigations of the stability of the optical fiber drawing process and its reaction to external disturbance, performed by the authors [10, 11], show that these two fundamental characteristics of the technological process depend substantially on the melt flow distribution along the length of the deformation zone. The most favorable temperature modes of fiber formation assuring both stability of the drawing process for practically any technically achievable values of the technological process parameters and minimal reaction of the fiber output diameter to external disturbances are indicated in [10]. The temperature mode of fiber formation is governed by the temperature distribution along the heating surface and by the temperature of the gas that is blown through the working space of the furnace [12]. In this connection, the temperature distribution over the length of ingot heating should satisfy conditions for the optimal temperature mode of fiber formation. It is here necessary to eliminate abrupt temperature gradients along the heating element surface since its failure is ordinarily caused not by overheating but by cracking of the working surface because of large thermal stresses in the material.

On the basis of the mass, momentum, and energy conservation laws, a foundation was given in [13] for a system of equations describing the behavior of a steady liquid jet of melted glass with a free surface during optical fiber formation:

Leningrad Institute of Precision Mechanics and Optics. Translated from *Inzhenerno-Fizicheski Zhurnal*, Vol. 54, No. 3, pp. 462-468, March, 1988. Original article submitted October 8, 1986.

$$\frac{1}{R^2} \frac{d}{dz} \left(3\mu_c R^2 \frac{dV}{dz} \right) - \rho_c V \frac{dV}{dz} + \rho_c g + \frac{1}{R^2} \frac{d\sigma R^2 H}{dz} = 0, \quad (1)$$

$$\frac{1}{R^2} \frac{d}{dz} \left(R^2 \lambda_{\text{qph}} \frac{dT}{dz} \right) - c_e \rho_c V \frac{dT}{dz} - \frac{2(1+R'^2)^{1/2}}{R} \alpha (T - T_g) +$$

$$+ \frac{4n_c^2 \sigma_0 (1+R'^2)^{1/2}}{R} \int_b^{b_1} \frac{R_{p1} (1+R_{p1}'^2)^{1/2} (\epsilon_p T_p^4 - \epsilon T^4)}{(z^* - z)^2 + (R_{p1} - R)^2} \cos \omega_1 \cos \omega_2 dz^* = 0,$$

$$H = \frac{\frac{1}{R} + \frac{1}{R} R'^2 - \frac{d^2 R}{dz^2}}{2(1+R'^2)^{3/2}}, \quad R_{p1}' = \frac{dR_{p1}}{dz^*}, \quad R' = \frac{dR}{dz}, \quad (2)$$

the remaining notation corresponds to the first part of the paper [14].

The system of equations (1)-(2) was solved numerically by the method of build-up under the following boundary conditions

$$V = V_{h1}, \quad T = T_{h1} \quad \text{for } z = b, \quad (3)$$

$$V = V_{h2}, \quad T = T_{h2} \quad \text{for } z = b_1. \quad (4)$$

The temperature distribution $T(z)$ along the length of the deformation domain and its corresponding jet shape of the melt $R(z)$ are found from the solution of the problem (1)-(4). The function $T_p(z)$ in (2) is selected by trial computations in such a way as to assure the optimal distribution $T(z)$ according to the recommendations given in [10]. The shape of the generator of the internal surface of the graphite heating element must be selected similar to the shape of the jet free surface (Fig. 1a): $R_{p1}(z) = R(z) + \delta$, which assures the maximal value of the angular radiation coefficients from the internal surface of the heater on the surface of the quartz glass melt.

A heat conduction equation for a resistive heater is formulated in [14] in which the intensity of the internal Joulean sources is described by the law $I^2 \nu_p / \pi^2 (R^2 - R_{p1}^2)$. Since the current intensity I and the function R_{p1} are given, then the distribution of the internal energy source intensity is determined by the function R_p . Therefore, the necessary temperature distribution T_p can be assured by an appropriate selection of the generatrix of the outer surface of the graphite heating element R_p .

The first approximation of the shape of the generatrix of the outer surface of the graphite heating element can be found from the equation

$$\frac{dR_p}{dz} = \frac{R_{p1}}{R_p} \frac{dR_{p1}}{dz} - \frac{1}{2R_p \lambda_p} \frac{dT_p}{dz} \left\{ \frac{I^2 \nu_p}{\pi^2 (R_p^2 - R_{p1}^2)} + \right.$$

$$+ \frac{d}{dz} \left(\lambda_p \frac{dT_p}{dz} \right) (R_p^2 - R_{p1}^2) - \xi_1 2R_p \left[2\sigma_0 n_c^2 R_{s1} (\epsilon_p T_p^4 - \epsilon_{s1} T_{s1}^4) \times \right.$$

$$\times \int_{a_3}^{a_4} \frac{\cos \theta_1 \cos \theta_2}{s_1^2} dz^* + \alpha_p (T_p - T_B) \left. \right] - \xi_2 2R_p \left[2\sigma_0 n_c^2 R_{sh} (\epsilon_p T_p^4 - \epsilon_{sh} T_{sh}^4) \times \right.$$

$$\times \int_{c_1}^{c_2} \frac{\cos \gamma_1 \cos \gamma_2}{s_4^2} dz^* + \alpha_p (T_p - T_B) \left. \right] - \xi_3 \frac{4\lambda_{sh} (T_p - T_{sh})}{\ln \frac{R_{sh}}{R_p}} -$$

$$- 2\alpha_{p1} R_{p1} (1 + R_{p1}'^2)^{1/2} (T_p - T_g) - 4R_{p1} (1 + R_{p1}'^2)^{1/2} \sigma_0 n_c^2 \times$$

$$\times \left[\xi_4 R_s (\epsilon_p T_p^4 - \epsilon_s T_s^4) \int_{c_3}^{c_4} \frac{\cos \varphi_1 \cos \varphi_2}{s_2^2} dz^* + \xi_5 \int_b^{b_1} (\epsilon_p T_p^4 - \epsilon T^4) \frac{\cos \omega_1 \cos \omega_2}{s_3^2} R (1 + R'^2)^{1/2} dz^* \right] \left. \right\}, \quad (5)$$

which is obtained from (1) in [14] under the assumption that $(dR_p/dz)^2 \ll 1$ and $\partial T_p / \partial \tau = 0$.

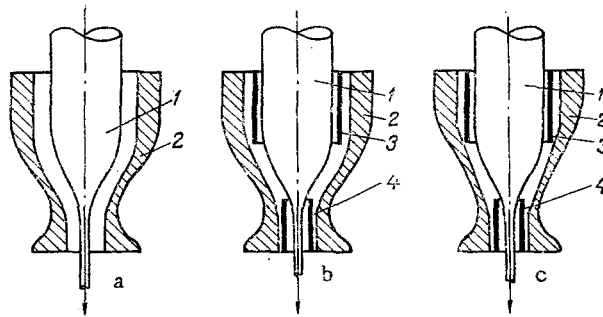


Fig. 1. Heating element of a resistive electrical furnace for drawing optical fiber. a) Without internal screens; b) with internal screens; c) with a conical internal surface shape for the heating element; 1) ingot; 2) heater; 3) upper screen; 4) lower screen.

The initial condition for this equation is found from the assumption of smallness of the quantity dR_p/dz for $z = a_1$. Assuming $dR_p/dz = 0$, a nonlinear equation in R_p can be obtained from (5) for $z = a_1$ from which the value of R_p is determined for $z = a_1$. The shape of the outer surface generatrix for the graphite heating element, found from the solution of (5) by the method of trial computations is refined by using a more exact algorithm which is considered in [14].

Thus, the method proposed above for optimizing the furnace construction can be represented as consisting of three fundamental blocks (Fig. 2). The first two subsystems were examined in detail upon and reduce to finding the functions R_{p1} , R_p and T_p that assure a diminution in the heater temperature, the temperature gradient along its surface, and the optimal temperature conditions for fiber formation from the solution of (1)-(4) and (5). The third subsystem (Fig. 2) permits optimization of the construction on the basis of an algorithm represented in [14]. This latter is achieved by a more accurate selection of the function $R_p(z)$ and a change in the structural features of the furnace.

The computations executed on the basis of solving the problem (1), (5)-(7) [14] permit making the following deductions: most optimal for localization of the heating zone and diminution of the temperature gradient along the heater surface is furnace construction in the presence of the upper 3 and lower 4 internal screens (see Fig. 1b). Moreover, the screens hinder incidence of graphite particles onto the ingot and the fiber being drawn, consequently, all the subsequent computation results are presented for heating an ingot in a furnace with internal screens.

Results of computing the shape of the jet and the temperature along its length are presented in Figs. 3 and 4 for the particular case of optical fiber formation from a 10 mm diameter ingot at a 0.5 m/sec drawing rate. Curve 1 in Fig. 3 corresponds to the jet shape while curves 2 and 3 correspond to the shape of the outer and inner heater surface generators. Curves 1 and 2 in Fig. 4 are referred to the temperature distribution in a quartz glass jet and along the heater surface. This latter is chosen so as to assure the necessary temperature distribution in the glass mass jet which is found from the solution of the boundary value problem (1)-(4). Smooth heating of the ingot in the domain A (Fig. 4) to a temperature somewhat above the temperature of the softening of the glass mass is assured for the thermal mode selected for the heating element. Rapid heating of the ingot to the temperature at which the glass flow reaches a value adequate for drawing a fiber occurs in the domain B, where the maximum of the glass mass temperature is reached in the lower part of the deformation domain (Figs. 3 and 4). Gradual cooling of the glass mass is observed in the domain C. According to [10], such a temperature distribution in the jet assures stability of the optical fiber drawing conditions and a minimal reaction to external disturbing effects for practically any technically attainable values of the technological process parameters for lightguide formation.

The shape of the inner surface generatrix for the graphite heating element is taken similar in shape to the jet surface, i.e., $R_{p1}(z) = R(z) + \delta$, where the quantity δ assures a definite 3 mm gap between the heater and jet surfaces. The glass mass is here heated to the requisite temperature at a lower maximal working temperature of the graphite heating element,

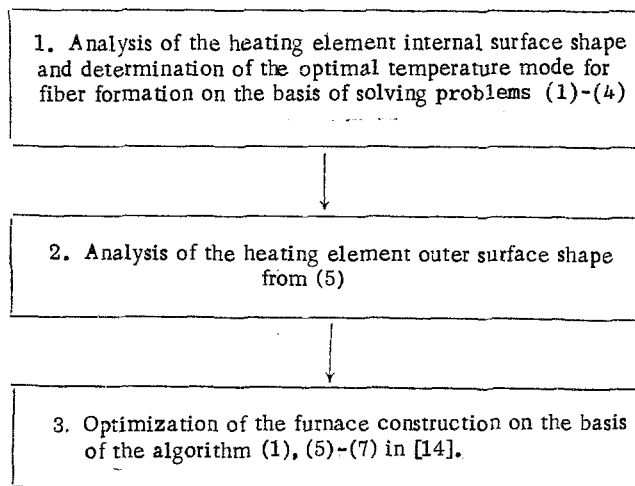


Fig. 2. Consolidated block diagram of the optimization algorithm for furnace construction.

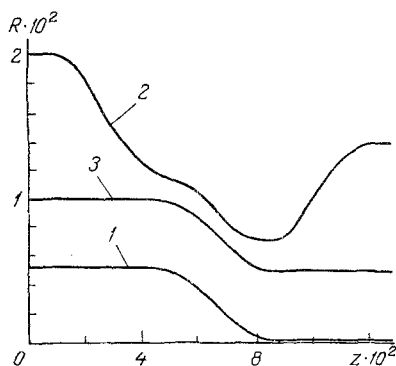


Fig. 3

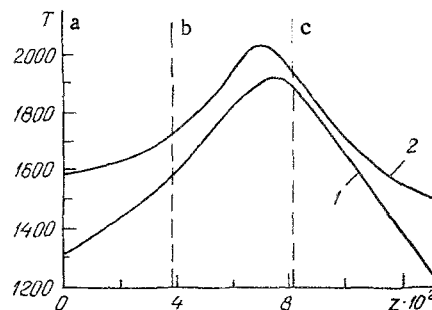


Fig. 4

Fig. 3. Shape of the jet surface generatrix (1), the outer (2) and inner (3) surfaces of the graphite heating element. R and z in m.

Fig. 4. Temperature distribution in the quartz glass jet (1) and along the heater surface (2). T , °C.

resulting in an increase in its exploitation time and a diminution in the dust particle concentration in the heating zone. The shape of the outer heating surface generator 2 (Fig. 3), obtained from the solution of the system (1), (5)-(7) from [14], as well as (5), assures the temperature distribution 2 (Fig. 4) along its surface for a 900-A current intensity.

From the viewpoint of simplifying the fabrication technology of the graphite heating element, the construction shown in Fig. 1c is more preferable. Here the shape of the heater inner surface is conical. Computations executed showed that all the positive qualities of the heating element construction (Fig. 1b) is also inherent to the heater with the conical internal surface.

In conclusion, it must be noted that the numerical computations confirm the possibility of active influence on the change in the temperature mode of the furnace by an appropriate selection of its structural (the presence or absence of internal screens, the quantity of external screens, the shape of the inner and outer heater surfaces, etc.) and the exploitational parameters (gas velocity and temperature at the entrance to the heating zone, current intensity flowing through the heating element).

NOTATION

μ_c , ρ_c , c_c , glass viscosity, density, and specific heat; V , velocity of the glass mass; g , free-fall acceleration; σ , surface tension coefficient; H , mean curvature of the jet surface; λ_{ef} , effective heat conduction coefficient of the glass mass; β , absorption coefficient;

δ , gas between the heating element surface and the jet surface; λ_p , heat conduction of graphite; R, R_p, R_{p1} , shapes of the jet surface generatrix, and the outer and inner heating element surfaces; a_i, b_j , respectively, the geometric dimensions of the furnace and the inner screen; R_{s1}, R_s , radii of the first outer and inner screens; T_p, T, T_{s1} and T_s , heater, jet, first outer, and upper or lower inner screen temperatures; z , longitudinal coordinate; I , current intensity passed through the heating element; ν_p , specific electrical resistivity of graphite; σ_0 , Stefan-Boltzmann constant; n_c , refractive index of the gas blown through the heating zone; $\epsilon, \epsilon_p, \epsilon_s, \epsilon_{s1}$, emissivity of the ingot, the heater, the inner screen, and the first outer screen; α_p , coefficient of external heat elimination from the outer heater surface; α, α_{p1} , local value of the coefficient of external heat elimination from the jet surface and the inner heater surface; T_g , a function that describes the longitudinal temperature distribution of the gas being blown through the heating zone; s_i , distance between the heat eliminating surfaces, $i = 1, 2, 3, 4$; V_{k1} , rate of ingot delivery into the heating zone; V_{k2} , rate of drawing fiber; T_{k1}, T_{k2} , temperatures on the boundaries of the computed areas; λ_{sh} , shell effective heat conduction; T_{sh} , shell temperature; R_{sh} , shell radius; ϵ_{sh} , shell emissivity, and τ , time.

LITERATURE CITED

1. D. N. Payne and W. A. Gambling, Am. Ceram. Soc. Bull., 55, No. 2, 195-197 (1976).
2. Prospectus of the firm "ASTRO," Optical Assembly HR-80, SK2465 (1980).
3. Prospectus of the firm "SENTORR," Optical Fiber Drawing Furnace 2A-100-SS, Model 11A (1982).
4. O. S. Gurvich, Yu. P. Lyakhin, and S. I. Sobolev, High-Temperature Furnaces with Graphite Elements [in Russian], Moscow (1974).
5. S. Sakaguchi, M. Nakahara, and Y. Tajima, Non-Cryst. Solids, 64(1, 2), 173-183 (1984).
6. S. M. Oh, Ceram. Bull., 58(11), 1108-1110 (1979).
7. F. T. Geylin, BSTJ, 55(8), 1011-1056 (1976).
8. É. N. Marmer and L. F. Mal'tseva, Élektrometriya, No. 5, 17-28 (1963).
9. V. K. Loksha, Problems of Thermal Energetics and Applied Thermophysics [in Russian], No. 5, Moscow (1966), pp. 164-175.
10. V. L. Kolpashchikov, Yu. I. Lanin, O. G. Martynenko, and A. I. Shnip, Influence of Drawing Temperature Modes on the Stability of Optical Fiber Parameters [in Russian], Preprint No. 12, Inst. Heat and Mass Transfer, Minsk (1984).
11. F. T. Geyling and C. M. Homsy, Glass Technol., 21, No. 2, 95-102 (1980).
12. V. S. Koren'kov, Hydrodynamics and Heat Transfer in Inhomogeneous Media [in Russian], Moscow (1983), pp. 66-71.
13. V. D. Naumchik, Energy Transfer in Convective Flows [in Russian], Minsk (1985), pp. 64-76.
14. V. N. Vasil'ev, G. N. Dul'nev, and V. D. Naumchik, Inzh.-Fiz. Zh., 54, No. 2, 248-256 (1988).